



### Design a Novel Fully Reconfigurable Nonreciprocal Quasi Reflectionless Microstrip Diplexer

Yasir M. Alabedi<sup>1</sup>, Seyed Vahab AL-Din Makki<sup>2</sup>, Nasr Alkhafaji<sup>1</sup>, Bahaa Hamzah Alkhuwaildi<sup>3</sup> and Sameer Al-Aljawad<sup>1</sup>, Ibtehal Farhan<sup>1</sup>

<sup>1</sup> Department of Communication Engineering Techniques, Engineering Technical College of Al-Najaf, Al-Furat Al-Awsat Technical University, Najaf, Iraq. E-mail: <a href="mailto:Yasir.alabedi@atu.edu.iq">Yasir.alabedi@atu.edu.iq</a>, <a href="mailto:nasrnomas@atu.edu.iq">nasrnomas@atu.edu.iq</a>, <a href="mailto:sameer.hadi@atu.edu.iq">sameer.hadi@atu.edu.iq</a> and <a href="mailto:ibtehalfarhan@gmail.com">ibtehalfarhan@gmail.com</a>

<sup>2</sup> Department of Electrical Engineering, Faculty of Engineering, Razi University, Kermanshah, Iran. E-mail: v.makki@razi.ac.ir

<sup>3</sup>Communications and Media Commission (CMC), Al-Furat Al-Awsat Office, Al-Najaf Al-Ashraf, Iraq.

E-mail: <u>bahaa.jasim.ms.etcn@student.atu.edu.iq</u> \*Corresponding author E-mail: <u>Yasir.alabedi@atu.edu.iq</u>

https://doi.org/10.46649/fjiece.v4.2.12a.24.9.2025

Abstract. In this paper, a novel design of a multifunctional quasi-reflectionless non-reciprocal diplexer is proposed. The reflection less diplexer is necessary to overcome many problems in various parts of communication systems that result from reflective unwanted signals from passive elements. in addition, the nonreciprocal diplexer has many advantages in RF systems as interference elimination. The proposed diplexer consists of two pseudocombline BPFs that work in two channels (2.2, 2.6) GHz, respectively. A T-shaped structure is used in the proposed QR diplexer design in three parts (an absorptive part for each BPF and a matching part between the two BPFs). Also the Spatial Temporal Modulation (STM) is used for achieving the nonreciprocity property for the diplexer. Furthermore, the proposed model achieved a high level of absorption for undesired reflected signals, where undesirable waves in the 1.5–4 GHz frequency band were efficiently absorbed. The proposed QR diplexer demonstrates a wide range of suppression for unwanted signals as well as significant separation between the RX and TX ports. All simulations are performed by Keysight ADS software and fabricated by a CNC machine. The results of the proposed work show good agreement between simulation and fabrication.

**Keywords:** multi-functional diplexer; reflectionless; non-reciprocal; diplexer; STM; reconfigurable diplexer.

#### 1. INTRODUCTION

Diplexers are crucial components in RF front-end circuits that work together with antennas to transmit and receive required signals. Also, it is a component having three ports that typically includes two microwave bandpass filters (BPFs) with different center frequencies. [1]. A diplexer is a component with three ports that can effectively divide and isolate distinct frequency bands. Additionally, it provides several additional uses for filters. This circuit is formed by interconnecting two filters with distinct resonant frequencies. Therefore, it is possible to use a single antenna as both a transmitter and receiver at the same time, while operating in distinct frequency ranges. A diplexer is a valuable analogue component used in the initial stages of telecommunications systems. As shown in Figure 1, the diplexer is positioned between the





antenna and the radio frequency section, which includes reception and transmittion. Conventional microwave diplexers in communications systems sometimes exhibit inadequate return loss (0 dB) in the stop frequency region, leading to the presence of undesirable signals in the receiver. Additionally, this leads to a decrease in the range of variability and a lack of consistency in telecommunications. Furthermore, because the power return takes place outside the intended frequency range, the use of strong amplifiers in satellites connected to these diplexers, terrestrial television broadcasting stations, and military and commercial radars may eventually cause physical harm and operational failure. The reflectionless structures possess the feature of having an optimal level of return loss in the stopband, which allows for the modification of the previous problems [2][3].

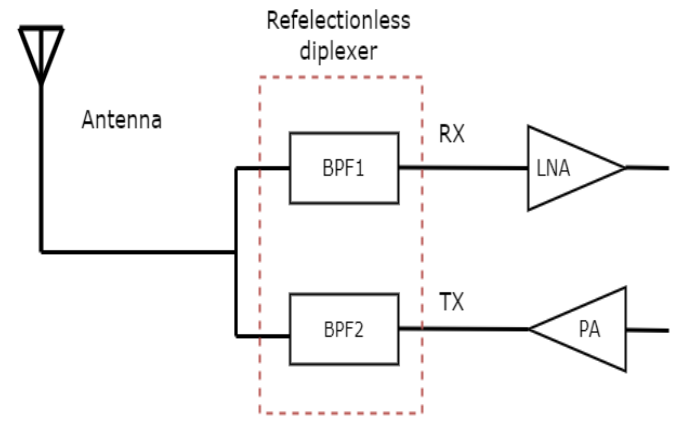


Fig. 1. Reflectionless diplexer placed in a telecommunication system.

In a diplexer, each channel's filter is an RF component designed to select a specific operating bandwidth while minimizing noise [4]. Conventional filters transmit in-band signals to the output port, while reflecting out-of-band signals back to the source [5]. To address this reflection, a new class of "reflectionless" or "absorptive" filters has been developed. These filters dissipate unwanted signals internally using lossy components, rather than reflecting them toward the input [6]. A conceptual circuit diagram of the reflectionless filter is shown in Figure 2.

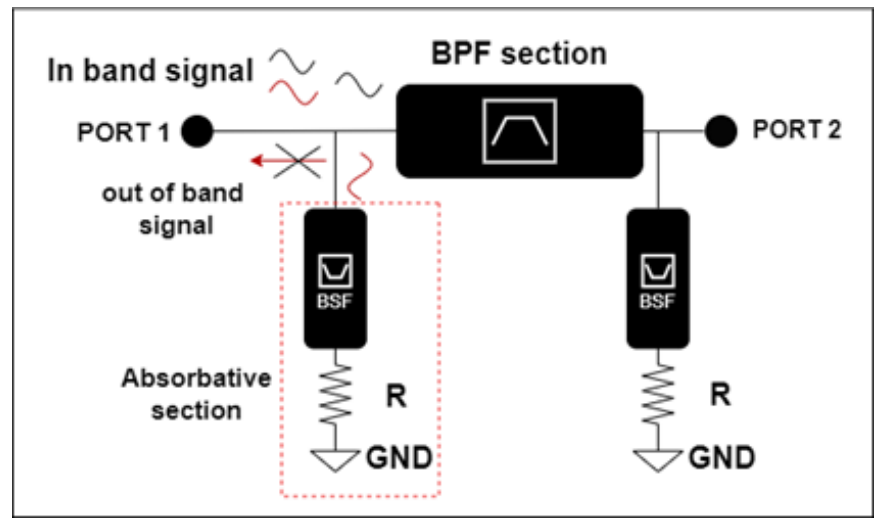


Fig. 2. Structure of the proposed quasi-Reflectionless bandpass filter.

Additionally, non-reciprocal devices, such as isolators and circulators, play a crucial role in the construction of communication systems. These devices are used to protect active components from





reflecting signals and/or eliminate the interference between the receive and transmit channels for full duplex communication [7-9]. Traditionally, non-reciprocal devices are implemented using ferromagnetic materials, which are known to be bulky and difficult to combine with other circuits [10-13]. [14]. Several research teams have reported the development of magnet-less nonreciprocal bandpass filters (BPFs) that utilize timemodulated resonators to enable unidirectional signal propagation ( $|S21| \neq |S12|$ ) [15–21]. The design of a completely reconfigurable multifunctional diplexer is presented in this study in order to improve the RF front-end's capabilities and minimize the size of RF front-end As seen in Figure 3, the non-reciprocity is achieved by applying the STM approach to the bandpass filters' (BPF) resonators with gradually phaseshifted AC signals. However, by using appropriate absorptive materials, the QR BPF can be attained.

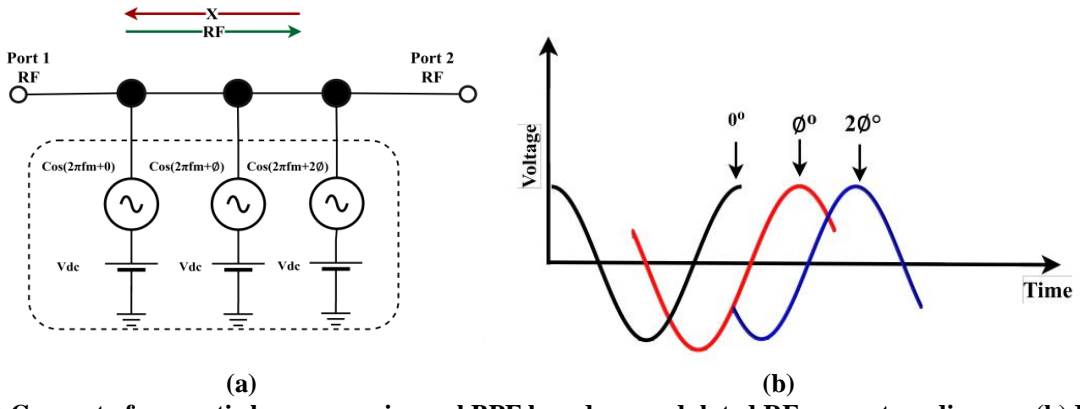


Fig. 3. (a) Concept of magnetic less non-reciprocal BPF based on modulated RF resonators diagram (b) Resonators Phase shifting.

#### 2. METHODOLOGY

This section is subdivided into four essential parts for designing the proposed diplexer. The first one is designing pseudocombline BPFs for both channels, while the second part is converting these two BPFs to a pseudocombline diplexer. Then, designing a proposed reflectionless pseudocombline diplexer, and at last STM technique and pin diodes are used with the QR diplexer to form the fully reconfigurable nonreciprocal QR diplexer.

#### 2.1. DESIGN OF PSEUDOCOMBLINE BPFS FOR BOTH CHANNELS

The first and second pseudocombline BPFs for the first and second channels (2.2 and 2.6) GHz will be designed using a coupling matrix. The construction of the pseudo-combline bandpass filter, which is made up of many connected resonators, is shown in Figure (4). Line components with numbers ranging from 1 to n make up the resonators. These line elements have a lumped capacitance Ci linked to the opposite end of each resonator line element and ground, and they are open-circuited at one end. Both the input and output of the filter use the tapped lines [22]. Certain transmission line lengths can be used in place of the capacitors.





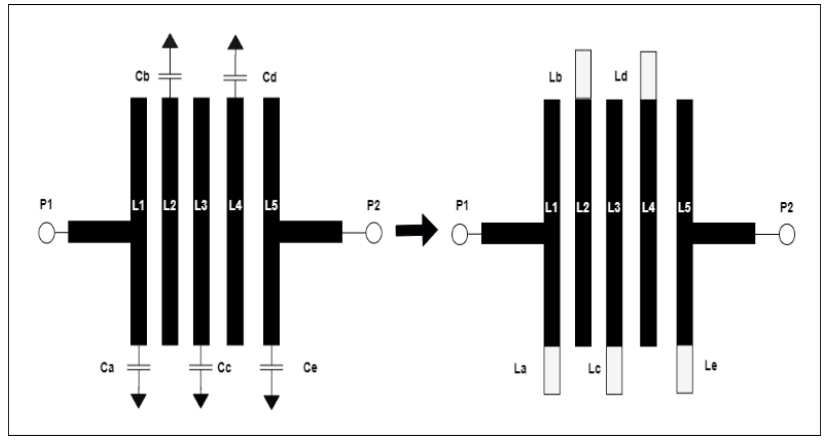


Fig. 4. Pseudocombline BPF structure.

To accomplish coupling fields fringes across neighbouring resonators with a separation of Si, i +1 for i = 1 - n - 1:

$$mi, j + 1 = \frac{FBW}{\sqrt{gigi + 1}} \tag{1}$$

$$FBW = \frac{f2-f1}{f0}$$
 ,  $fo = \sqrt{f1f2}$ 

The center frequency is fo, while the upper and lower resonant frequencies are f1 and f2, respectively, and the ladder-type lowpass prototype filter's element values are denoted by gi and gi+1. The filter's normalized cut off frequency is at  $\Omega c = 1$ . From (1), the mutual coupling matrix (M) may be computed. It is possible to ascertain the true filter dimensions of both BPFs (w1, w2,... w5, s0,1, s1,2, s2,3, s3,4, s4,5) [15]. The fractional bandwidth is denoted by FBW. Depending on the values in Table 1 and the coupling matrices below (M1 and M2), the first and second BPFs may be built to achieve the first and second channels (2.1, 2.5 GHz).

	Table 1: I arameter design of both B1 1's							
ſ	Domomotoma	fo	$f_1$	$f_2$	FBW	BW		
	Parameters	(GHz)	(GHz)	(GHz)	GHz)	(MHz)		
	BPF 1	2.1	1.93	2.31	0.18	380		
	BPF 2	2.5	2.45	2.7	0.097	250		

$$M1 =$$

ΓO	0.5	0	0	0	0	0 ]	
0.5	0	0.153	0	0	0	0	
0	0.153	0	0.109	0	0	0	
0	0	0.109	0	0.109	0	0	
0	0	0	0.109	0	0.153	0	
0	0	0	0	0.153	0	0.5	
Lo	0	0	0	0	0.5	0 1	

$$M2 =$$

Γ0	0.3	0	0	0	0	0 ]
0.3	0	0.082	0	0	0	0
0	0.082	0	0.058	0	0	0
0	0	0.058	0	0.058	0	0
0	0	0	0.058	0	0.082	0
0	0	0	0	0.082	0	0.3
Lo	0	0	0	0	0.3	0 7





Analytical S-parameters for both BPFs that can be obtained from coupling matrices (M1 and M2) depend on the parameters mentioned in Table 1, shown in Figure 5.[23]

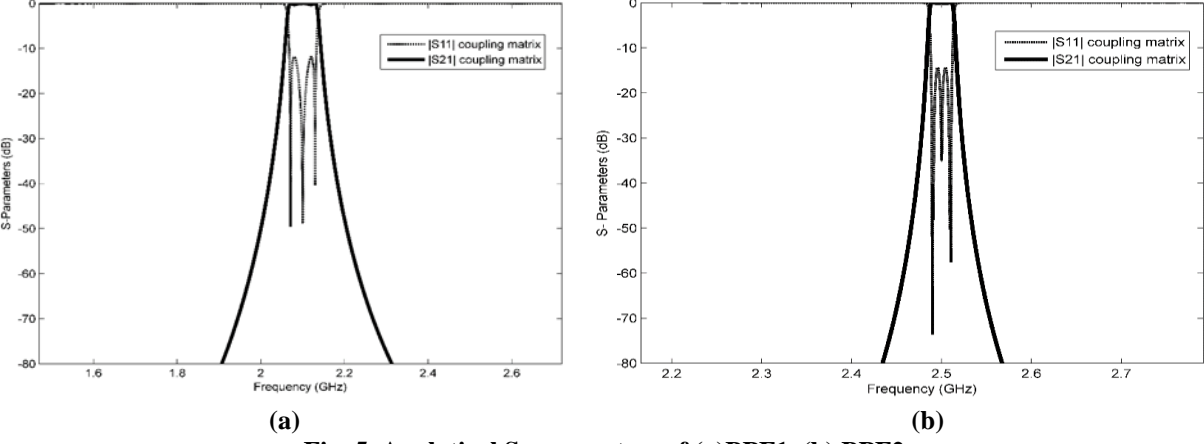


Fig. 5. Analytical S-parameters of (a)BPF1, (b) BPF2.

The actual widths and lengths of the first and second BPFs can be obtained and optimized using ADS tools, as shown in Tables 2 and 3. The layout for both filters is shown in Figure 6. The feeding location (FL) is denoted by the electrical distance (Lt) from the shorted end of the input/output resonator [13].

$$Lt = \frac{2Lr}{\pi} \sin^{-1}\left(\sqrt{\frac{\pi Zo}{2Q_{\theta} Zf}}\right) \tag{2}$$

Zo symbolizes the transmission line's characteristic impedance, which produces the interdigital bandpass filter (BPF) resonator.whereas Zf represents the characteristic impedance of the transmission line used for feeding the input and output.

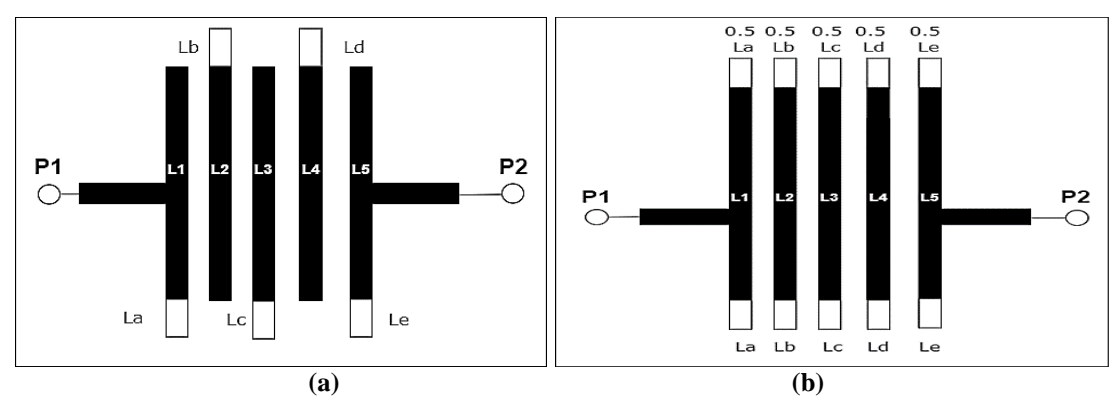


Fig. 6. Structure of first and second BPFs (a) BPF1 (b) BPF2 (Deign parameters of BPF1 are FL = 28.91, L1=20.45, L2=17.91, L3=17.83, W= 2.39, WF=1.85 LF=11.5, La=17.85, Lb=19.45, Lc=20.68, Ld=20.6, Le=21.98, Wa=2.39, Wb=2.39, Wc=2.29, Wc=2.29, Wc=2.29, Wc=2.29, Wc=2.29, Wc=2.29, Wr=2.39, WF=2.39, WF=2.39, Ld=2.39, Ld=2.39, Ld=2.39, Wc=2.39, Wc=2.39

Figure 7 demonstrates that the feeding location (FL) is crucial in determining how to regulate the external quality component.





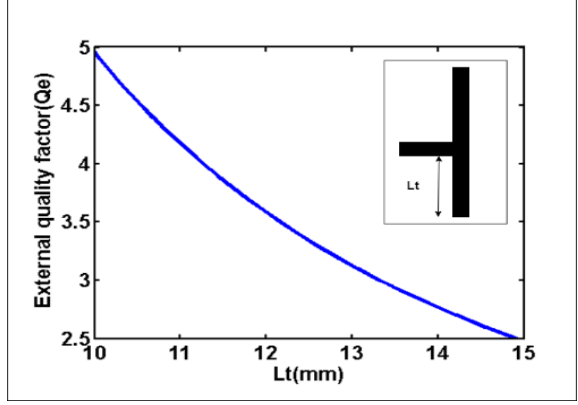


Fig. 7. Design curves (external quality factor) for designing the pseudocombline BPF.

The exterior quality factor decreases as Lt increases. The amount of input power that may be supplied to the resonator reduces as its length (Lt) increases. Figure 8 displays the two bandpass filters' (BPFs') simulated S-parameters. For both bandpass filters (BPFs), the simulated S-parameters nearly match the analytical results. The first BPF's center frequency is 2.2 GHz, while the second BPF's center frequency is 2.6 GHz.

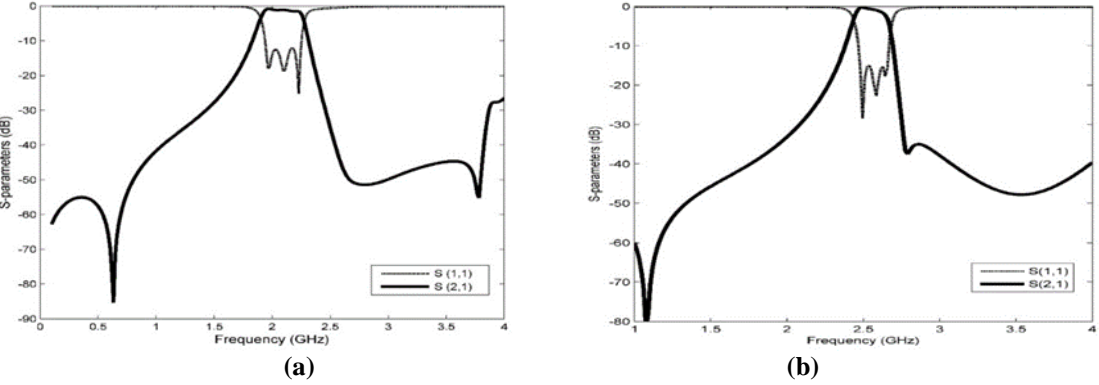


Fig. 8. Simulated S-parameters of (a) BPF1, (b) BPF2.

The magnitude of return loss for both BPFs is shown in Figure 9. It's clear that the level of return loss in out-of-band Reagans is high; this harms other circuit elements.

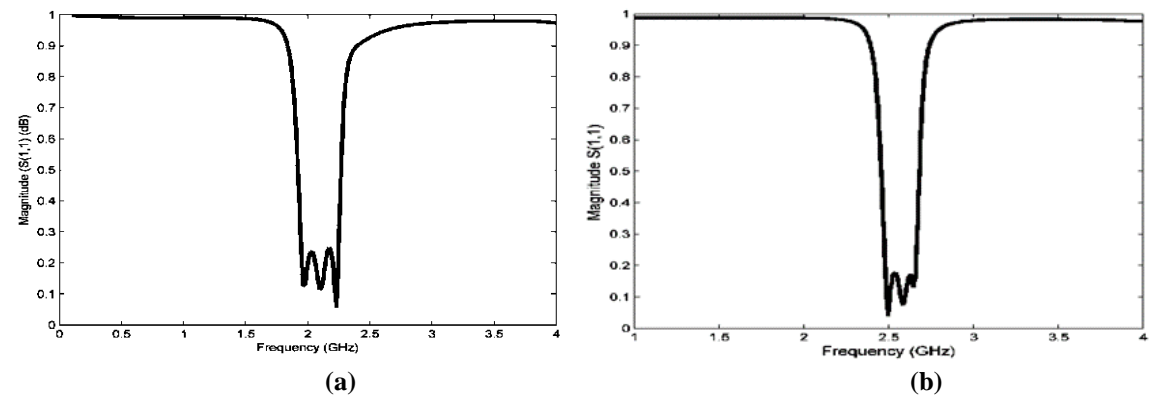


Fig. 9. Simulated magnitude of return loss for (a) BPF1, (b) BPF2.





#### 2.2. DESIGN OF PSEUDOCOMBLINE DIPLEXER

A reflective pseudo-combline diplexer formed of two BPFs will be designed in this subsection. The first and second BPFs that were designed in the previous subsection can be combined to form the reflective diplexer. However, the matching level is impacted by the combined action of these two filters, which changes the diplexer's frequency response. Consequently, after combining these two bandpass filters, a change is required. When two filters are combined, they can employ a T-shaped section between them and their input ports will become shared. Table 2 displays the dimensions of the suggested diplexer, while Figure 10 depicts its general structure.

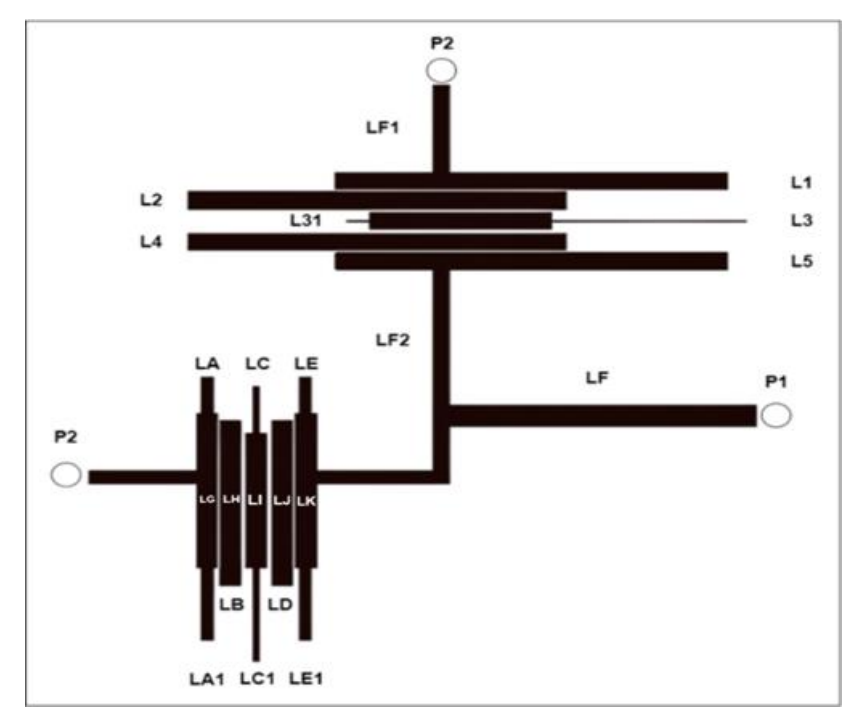


Fig. 10. Overall structure of proposed diplexer.

Table 2. Parameter design of the proposed diplexer.

Table 2. Parameter design of the proposed diplexer.						
LF	LF1	Ll	F2	L1	L2	L3
11.5	32.89	17	.82	41.9	40.52	20.73
L4	L5	L	A	LB	LD	L31
40.52	41.9	4.	97	22	22	2.5
LE	LE1	L	<b>A</b> 1	LJ	LK	LC
4.79	9.58	9.58		22	20.45	6.22
LG	L33		S1	,2=S4,5	S2,3=S3,4	LC1
20.45	19.56	<u> </u>		0.13	0.36	12.45

S-parameters and isolation of the proposed diplexer are shown in Figure 11.





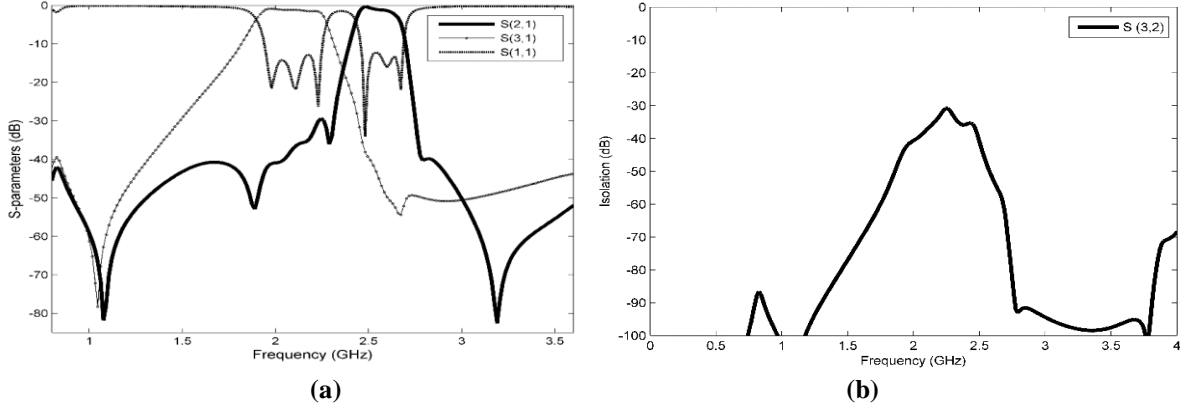


Fig. 11. (a) Simulation S-parameters of the proposed diplexer, (b) Magnitude of isolation.

It's clear that the center frequencies for both BPFs are (2.2,2.6) GHz and the isolation between the TX and RX ports is better than 30 dB, also the magnitude of reflective ratio for proposed reflective diplexer shown in figure (12), where it have a high level in out of band regions, this harm another circuit elements as mention above.

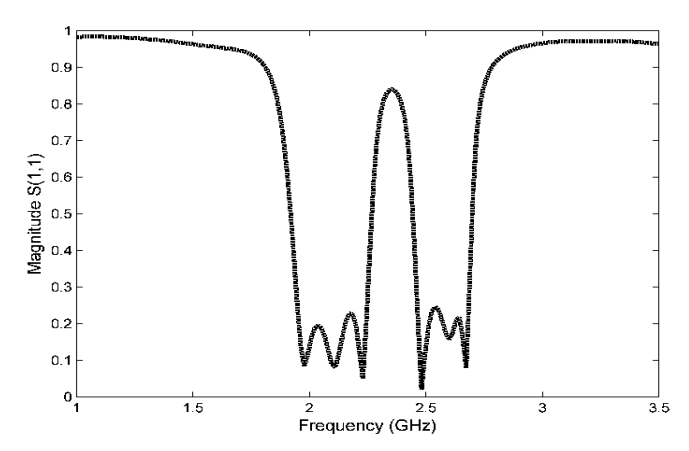


Fig. 12. The magnitude of the reflective ratio for the proposed reflective diplexer.

#### 2.3. DESIGN OF QUASI REFLECTIONLESS PSEUDOCOMBLINE DIPLEXER

For obtaining a reflectionless response for the proposed diplexer, a suitable T-shaped absorber must be designed for both BPFs in this subsection. Where the two absorptive acts as BSFs at the resonant frequencies depend on the complementary diplexer concept that is used in reflectionless designs, as shown in Figure 13.





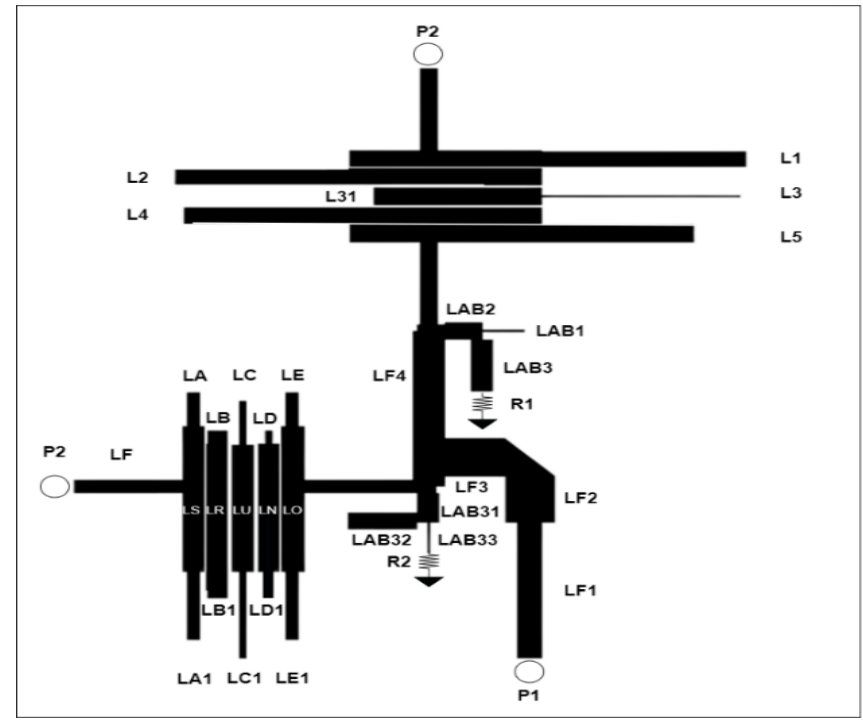


Fig. 13. Overall structure of proposed reflection less diplexer.

Each absorber can absorb signals at specific frequencies where it matches with each BPF. As shown in this figure, there is a resistor element connected at the end of each absorber, where it can absorb unwanted signals. The first absorptive acts as BSF in the first channel frequency, as well as the second absorptive. T-shaped absorptive can be designed and connected for both BPFs, with a connecting lumped resistor at their other end as shown in Figure 14-b).

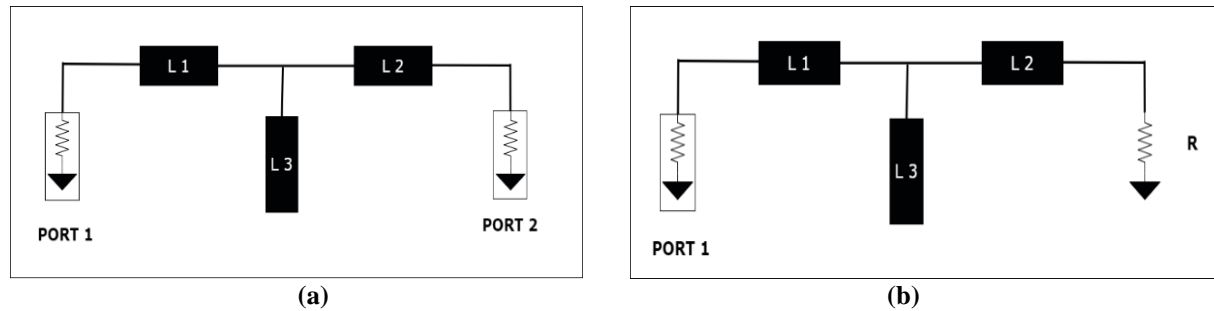


Fig. 14. (a) Structure for BSF (b) Absorptive structure.

A T-shaped section can be used as a matching section between the two BPFs. The structure of T-absorptive parts for both channels is shown in Figure 14-a. Where the parameters of the first absorptive (L1 = L2 = 19.5, w1 = 1.1, w2 = 2.1, L3 = 19.2, w3 = 1 mm, also, for the second one are (L1 = 12, L2 = 15.5, L3 = 19.5, w1 = 1.1, w2 = 2.1, w3 = 1 mm.

S-parameters for both BSFs are shown in Figure 15, where the center frequencies for both BSFs are (2.2, 2.6) GHz, respectively. These BSFs are connected to both channels for absorbing unwanted signals, as shown in Figure 16.





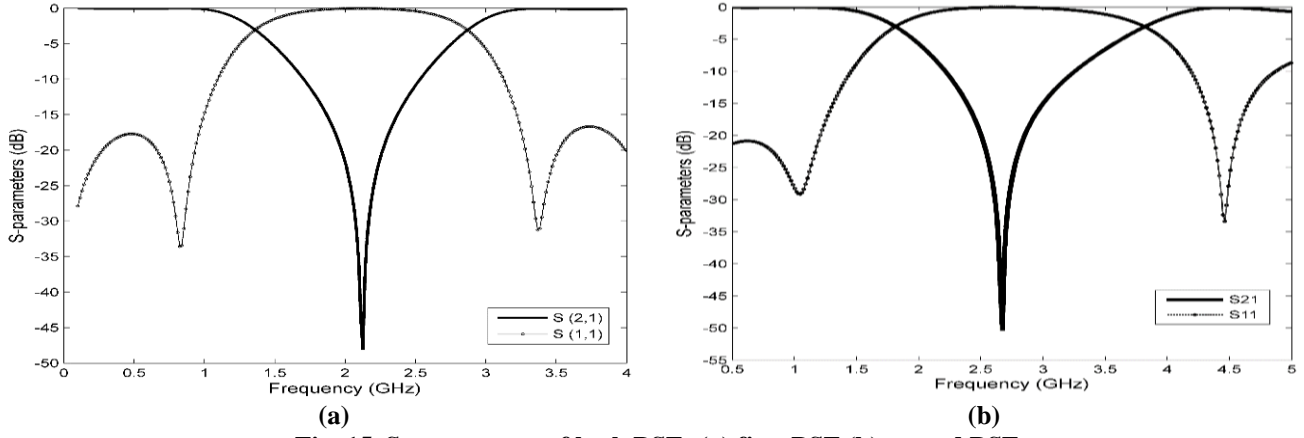


Fig. 15. S-parameters of both BSFs (a) first BSF (b) second BSF.

The two absorptive are connected at these places, depending on the current distribution shown in Figure 17. At the two resonant frequencies, the current distribution at those places is high, and this will increase the absorptive rate for a reflective signal.

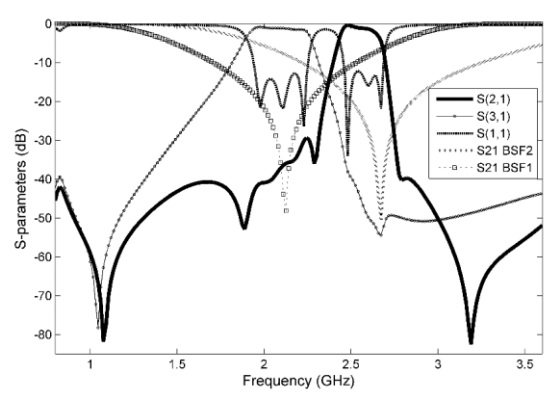


Fig. 16. S-parameters of both BSFs and BSFs.

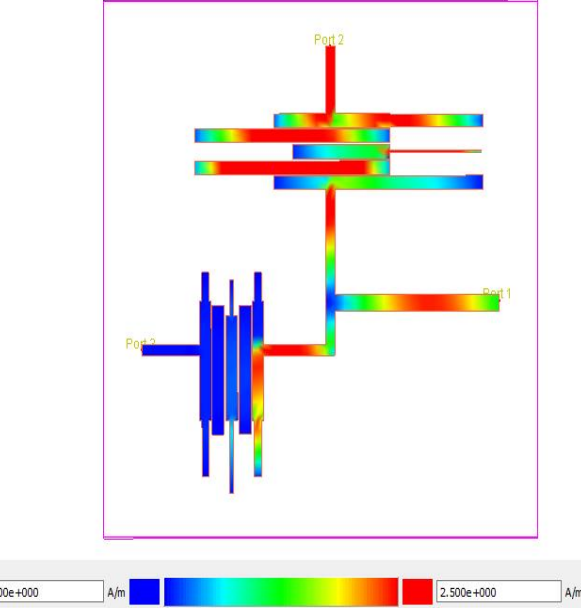


Fig. 17. Current distribution of proposed reflectionless diplexer.





The simulated S-parameters of the reflectionless diplexer are shown in figure 18-a) depending on the parameter design in Table 3. As can be seen, the return loss is lower than 3dB at a wide range of frequencies for both channels. Also, the absorbing ratio is shown in figure 18-b), as can be seen in this figure, the absorbing ratio increases in the band regions of each BPF, as well as out of band for each one.

Table 3. Parameters design of fabrication proposed QR diplexer (mm).

LF	LF1	LF2	LF3	LF4	L1
11.5	17.37	7.78	7.78	13	41.83
L2	L3	L31	L4	L5	LA
38.61	20.68	17.83	37.56	37.9	4.74
LB	LC	LD	LE	LA1	LB1
1.87	6.07	1.87	4.74	9.48	3.74
LC1	LD1	LE1	LS	LR	LU
12.15	3.74	9.48	20.45	17.91	17.83
LN	LO	LAB1	LAB2	LAB3	LAB31
17.91	20.45	4.42	4.1	7.35	4.1
LAB32	LAB33	S1,2=S 4,5	S2,3=S 3,4	R1	R2
7.35	4.25	0.13	0.36	50 Ω	200 Ω

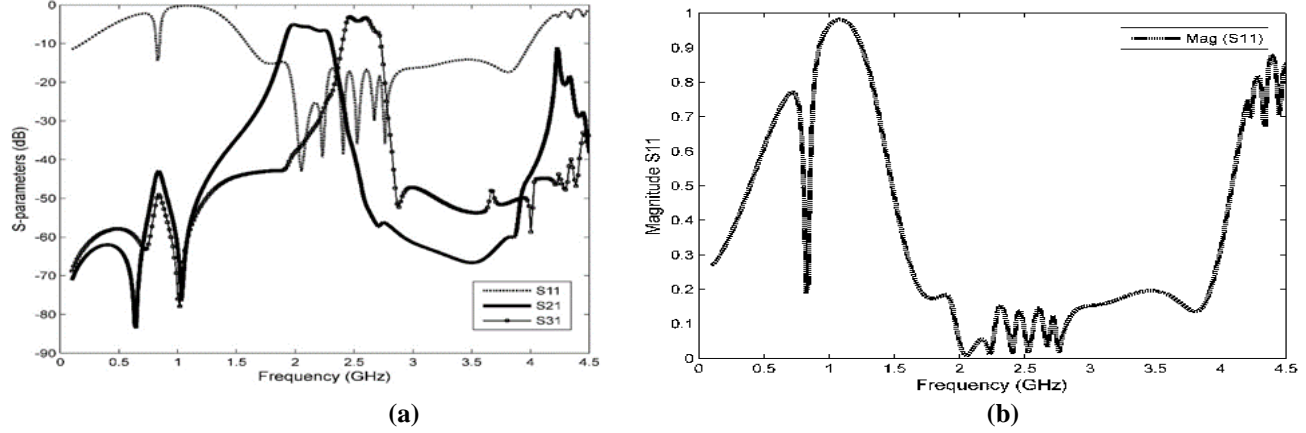


Fig. 18. Simulated results of reflectionless diplexer (a) S-parameters, (b) absorbing ratio.

#### 3. DESIGN OF FULLY RECONFIGURABLE MULTIFUNCTIONAL DIPLEXER (FRMD)

In this section, a novel multi-function will be developed for the first time. The information provided in the preceding chapters will be utilized to design a multifunctional and reconfigurable diplexer (FRMD) that may provide various responses based on the desired purpose. This design enables the development of a component that can effectively handle multiple functions and features necessary for enhancing the performance of front-end devices. It possesses the capability to prevent the reflection of unwanted signals and interference in both receivers and transmitters, as previously explained. The architecture of the proposed diplexer is illustrated in Figure 19; the parameters for designing FRMD are indicated in Table 4.

Table 4. Parameters design of fabrication proposed QR diplexer (mm).

LF	LF1	LF2	LF3	LF4	L1
11.5	13.13	12.21	0.99	16.91	42.4
L2	L3	L31	L4	L5	LA
38.51	20.68	17.83	37.36	38.3	4.69
LB	LC	LD	LE	LA1	LB1
0.37	6.12	0.37	4.69	9.38	0.74



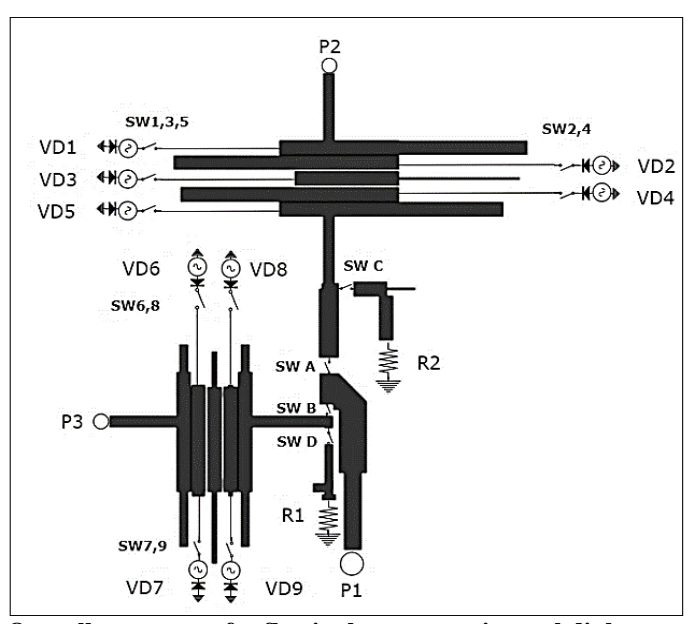


LC1	LD1	LE1	LS	LR	LU
12.25	0.74	9.38	20.45	17.91	17.83
LN	LO	LAB1	LAB2	LAB3	LAB31
17.91	20.45	4.82	5.7	7.55	6.8
LAB32	LAB33	\$1,2=\$4 ,5	S2,3=S3,4	R1	R2
2	1.34	0.129	0.36	50 Ω	150 Ω

This proposed diplexer possesses the capability to provide 8 distinct responses, which vary depending on its intended use. Additionally, it may be controlled through the utilization of switches (pin diodes).

- 1- The proposed design can operate as a traditional bandpass filter. It allows the first channel to pass through only when switch A is activated and all other switches are deactivated. This can be observed in Figure 20-a.
- 2- The second paragraph of the table indicates that activating the second channel requires the activation of switch B while deactivating all other switches. This is illustrated in Figure 20-b.
- 3- The proposed design functions as a conventional diplexer with a reflective characteristic. This is achieved by connecting switches A and B while deactivating the remaining switches, as illustrated in Figure 20-c).
- 4- The proposed design functions as a standard diplexer with a reflection less characteristic. This is achieved by activating switches A, B, C, and D, which connect the absorbing components. The outcome of this configuration is illustrated in Figure 20-d.
- 5- The proposed design has a non-reciprocal characteristic that effectively prevents interference by inhibiting propagation in two opposing directions. To achieve this, switches a and b are operated on, and switches 1-5 and 6-9 are connected, as depicted in Figure 20-e).
- 6- The non-reciprocal response can be achieved for the first channel of the diplexer by activating switches a, b along with switches 1 to 5, as seen in Figure 20-f).
- 7- The non-reciprocal response can be achieved for the second channel by activating switches a, b, and switches 6 to 9, as depicted in Figure 20-g.

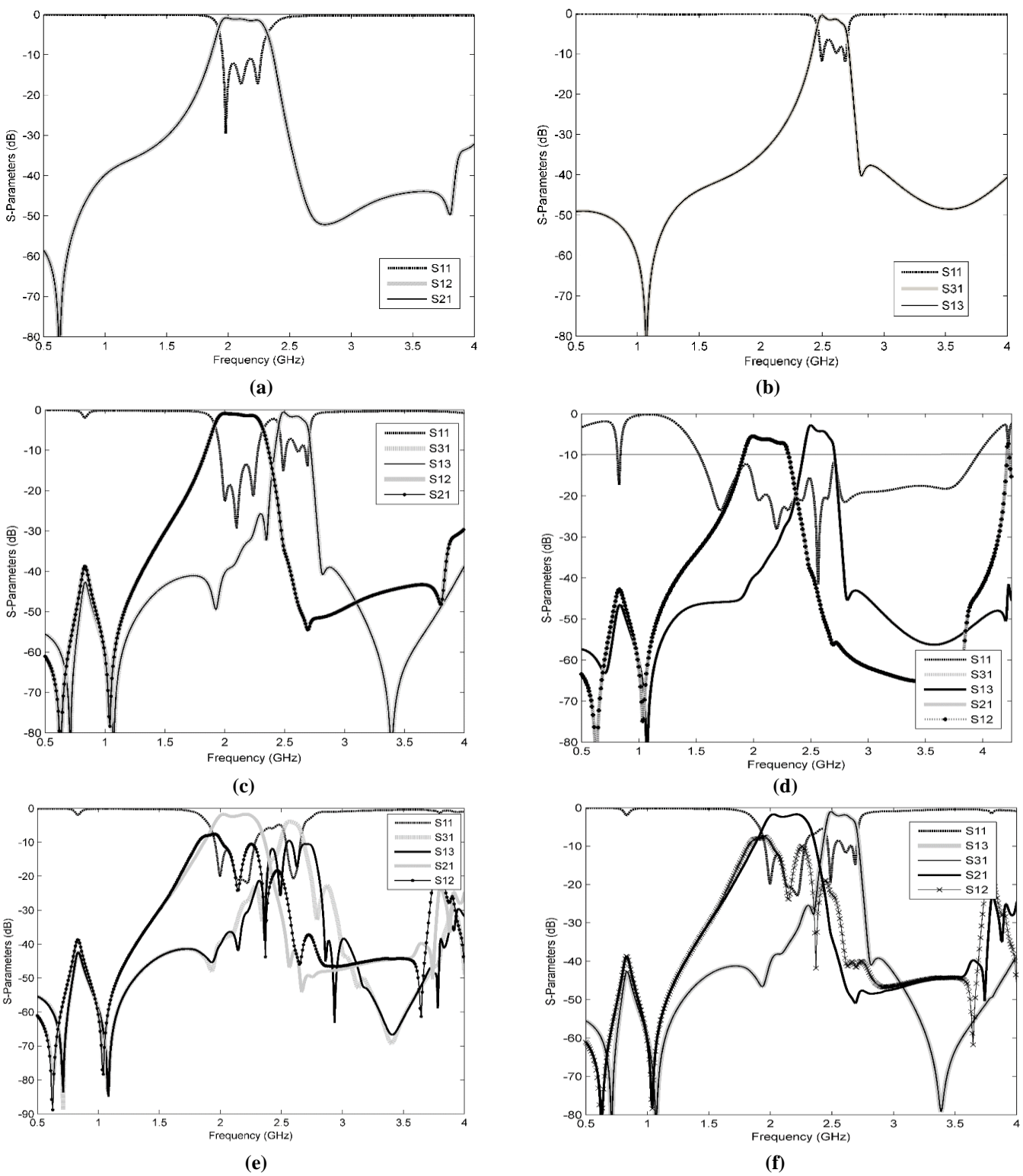
To achieve a diplexer response that is reflection less and non-reciprocal, all switches must be turned on. As it's clear in Figure 20-h.



 $Fig.\ 19.\ Overall\ structure\ of\ reflectionless\ non-reciprocal\ diplexer.$ 

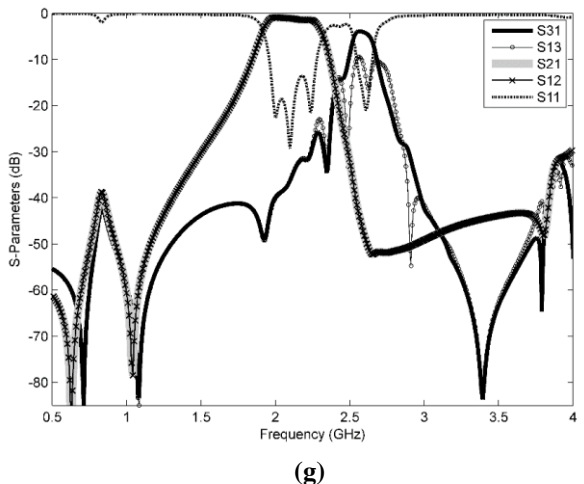












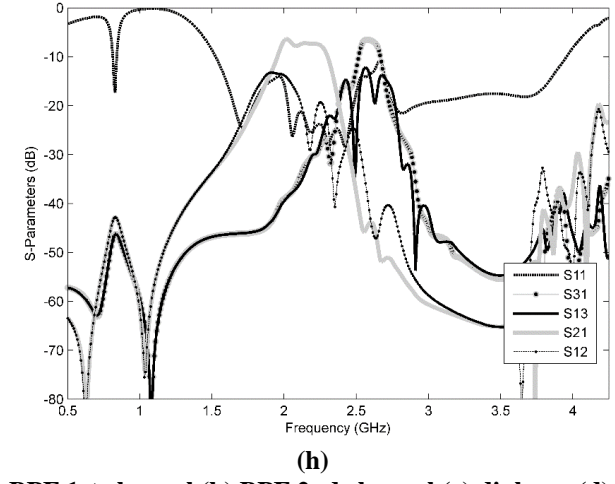


Fig. 20. All S-parameters response of proposed (FRMD) (a) BPF 1st channel (b) BPF 2nd channel (c) diplexer (d) QR diplexer (e) Non reciprocal diplexer (f) 1st channel Non reciprocal diplexer (g) 2nd channel Non reciprocal diplexer (h) QR Non reciprocal diplexer.

#### 4. STATE OF ART

In this chapter, we will compare our work with similar studies from recent years, focusing specifically on the degree of unwanted signal coupling in the diplexer. As shown in table 5.

Table 5. Parameters design of fabrication proposed QR diplexer (mm).

No.	Ref.	Freq.	Multifunctional	Reflection-less range (10dB) (GHZ)
1	[20]	1.7,2	NO	1.3 - 2.4
2	[21]	1.7,2	NO	1.5 - 3
3	THIS WORK	2, 2.6	YES	1.5 - 4

From the previous comparison, it is clear that the proposed model outperforms most previous studies in its ability to absorb unwanted reflected signals. It is also distinguished by being one of the few works with multifunctional capability, as it can simultaneously absorb undesired signals and perform bidirectional transmission isolation at the same time — a feature not found in other models presented in earlier research. Moreover, according to the authors' knowledge, there are only a limited number of studies addressing this specific topic.

#### 5. EXPERIMENTAL VALIDATION

The first step involves designing, simulating, fabricating, and measuring QR pseudocombline diplexer in order to validate the suggested design. The dielectric loss tangent  $\tan(\delta D) = 0.017$ , the dielectric thickness h = 1.5 mm, and the relative dielectric constant  $\epsilon r = 4.6$  are all present in a FR4 substrate. The diplexer operates at frequencies of 2.1 and 2.65 GHz. Additionally, the schematic and EM designs are analyzed and implemented using the Keysight Advanced Design System software (ADS). observing the design process. A CNC machine is used for the fabrication. A Keysight N9917A microwave analyzer was used to experimentally assess their RF performances in terms of S-parameters. The suggested diplexer's





measurement procedure is depicted in Figure 21. Figure 22 displays the measurement S-parameters for the suggested diplexer. Both bands have center frequencies of 2.2 and 2.6. There is 30 dB of isolation between the TX and RX ports. As anticipated, the absorbing ratio is also for the wide band.



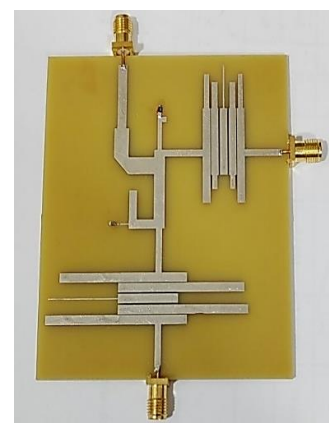
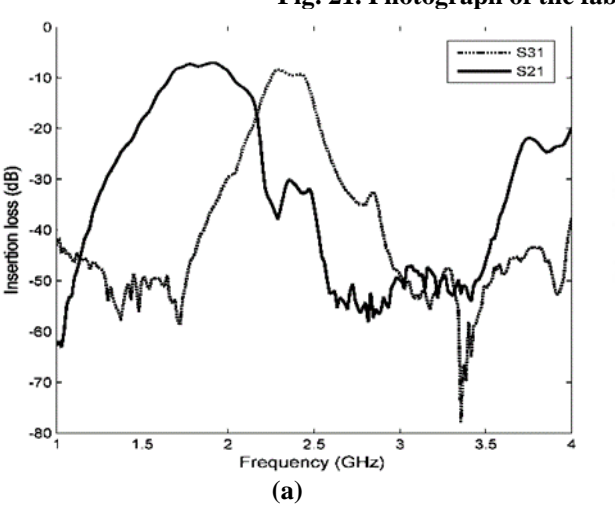


Fig. 21. Photograph of the fabricated proposed QR diplexer.



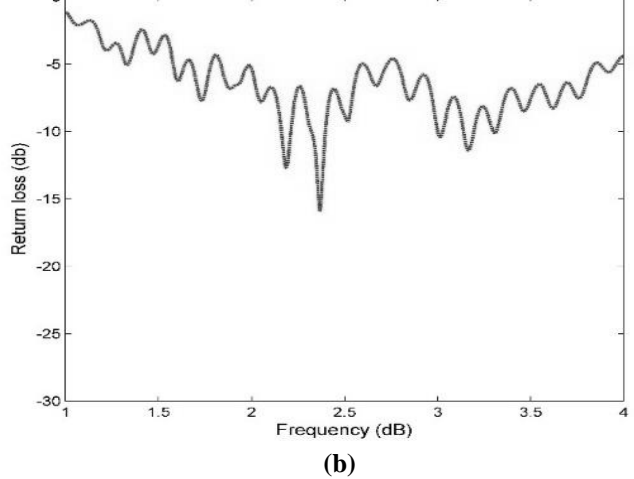


Fig. 22. Measurement results of reflectionless diplexer (a) Insertion loss (b) Return loss.

#### 6. CONCLUSION

In this paper, a novel fully reconfigurable quasi reflectionless nonreciprocal design is presented. As mentioned above, there is an essential need to decrease the effect of unwanted signals at regions of in and out of bands for both channels, as well as the elimination of the interference inside the diplexer. Therefore, the first stage of this paper was to design two BPFs for both channels and measure the absorptive ratio at out-of-band regions. After that, two absorptive parts are designed for both channels to absorb the unwanted signals for both channels. QR diplexer can be designed by connecting these two absorptive with a diplexer. Also, varactor diodes are added for modulation purposes to achieve the nonreciprocity goal. The proposed QR diplexer was designed using Advanced Design System (ADS) and fabricated by a CNC machine, it was also fabricated using an FR4 substrate and measured in order to validate the proposed design. By comparing the simulation with the measured results, it's clear that they are in good agreement.





#### **REFERENCES**

- [1] J. K. Xiao, Y. Li, M. Zhu, W. Zhao, L. Tian, and W. J. Zhu, "High selective bandpass filter with mixed electromagnetic coupling and source-load coupling," AEU Int. J. Electron. Commun., vol. 69, no. 4, pp. 753–758, 2015.
- [2] A. Taghvaei, R. Bayderkhani, and M. Espahbodi, "Design and Fabrication of Adjustable Reflectionless Microstrip Diplexer for L-Band," Prog. Electromagn. Res. C, vol. 126, no. November, pp. 173–181, 2022.
- [3] Morgan, M. A., Reflectionless Filters, Artech House, 2017.
- [4] X. Wu, Y. Li, and X. Liu, "Quasi-Reflectionless Microstrip Bandpass Filters with Improved Passband Flatness and Out-of-Band Rejection," IEEE Access, vol. 8, pp. 160500–160514, 2020.
- [5] M. A. Morgan, "Think outside the band: Design and miniaturization of absorptive filters," IEEE Microw. Mag., vol. 19, no. 7, pp. 54–62, 2018.
- [6] K. Da Xu, S. Lu, Y. J. Guo, and Q. Chen, "Quasi-Reflectionless Filters Using Simple Coupled Line and T-Shaped Microstrip Structures," IEEE J. Radio Freq. Identif., vol. 6, pp. 54–63, 2022.
- [7] D. M. Pozar, Microwave Engineering. Wiley, 2012.
- [8] Z. Yong, Z. Jian, Y. Yuanwei, C. Chen, and J. S. Xing, "A Ku-Band Novel Micromachined Bandpass Filter with Two Transmission Zeros," no. August, 2013.
- [9] J. Zhou, N. Reiskarimian, J. Diakonikolas, T. Dinc, T. Chen, G. Zussman, and H. Krishnaswamy, "Integrated full duplex radios," IEEE Communications Magazine, vol. 55, no. 4, pp. 142–151, April 2017.
- [10] A. Kord, D. L. Sounas, and A. Alu, "Achieving full-duplex 'communication: Magnetless parametric circulators for full-duplex communication systems," IEEE Microwave Magazine, vol. 19, no. 1,pp. 84–90, Jan 2018.
- [11] C. E. Fay and R. L. Comstock, "Operation of the ferrite junction circulator," IEEE Transactions on Microwave Theory and Techniques, vol. 13, no. 1, pp. 15–27, Jan 1965.
- [12] S. A. Oliver, P. Shi, N. E. McGruer, C. Vittoria, W. Hu, H. How, S. W. McKnight, and P. M. Zavracky, "Integrated self-biased hexaferrite microstrip circulators for millimeter-wavelength applications," IEEE Transactions on Microwave Theory and Techniques, vol. 49, no. 2, pp. 385–387, Feb 2001.
- [13] C. K. Seewald and J. R. Bray, "Ferrite-filled antisymmetrically biased rectangular waveguide isolator using magnetostatic surface wave modes," IEEE Transactions on Microwave Theory and Techniques, vol. 58, no. 6, pp. 1493–1501, June 2010.
- [14] X. Wu, M. Nafe, A. A. Melcón, J. Sebastián Gómez-Díaz and X. Liu, "A Non-Reciprocal Microstrip Bandpass Filter Based on Spatio-Temporal Modulation," 2019 IEEE MTT-S International Microwave Symposium (IMS), Boston, MA, USA, 2019, pp. 9-12.
- [15] N. A. Estep, D. L. Sounas, and A. Alù, "Magnetless microwave circulators based on spatiotemporally modulated rings of coupled resonators," IEEE Trans. Microw. Theory Techn., vol. 64, no. 2, pp. 502–518, Feb. 2016.
- [16] A. Kord, D. L. Sounas, Z. Xiao, and A. Alu, "Broadband cyclicsymmetric magnetless circulators and theoretical bounds on their bandwidth," IEEE Trans. Microw. Theory Techn., vol. 66, no. 12,pp. 5472–5481, Dec. 2018.
- [17] A. Kord, D. L. Sounas, and A. Alù, "Pseudo-linear time-invariant magnetless circulators based on differential spatiotemporal modulation of resonant junctions," IEEE Trans. Microw. Theory Techn., vol. 66, no. 6, pp. 2731–2745, Jun. 2018.
- [18] X. Wu et al., "Isolating bandpass filters using time-modulated resonators," IEEE Trans. Microw. Theory Techn., vol. 67, no. 6, pp. 2331–2345, Apr. 2019.
- [19] D. Simpson and D. Psychogiou, "Magnet-less non-reciprocal bandpass filters with tunable center frequency," in Proc. 49th Eur. Microw. Conf.





(EuMC), Oct. 2019, pp. 460-463.

- [20] D. Simpson and D. Psychogiou, "Fully-reconfigurable non-reciprocal bandpass filters," in IEEE MTT-S Int. Microw. Symp. Dig., Aug. 2020,pp.807–810.
- [21] A. Alvarez-Melcon, X. Wu, J. Zang, X. Liu, and J. S. Gomez-Diaz, "Coupling matrix representation of nonreciprocal filters based on timemodulated resonators," IEEE Trans. Microw. Theory Techn., vol. 67, no. 12, pp. 4751–4763, Dec. 2019.
- [22] Hong, Jiasheng & Lancaster, M. (2001). Microstrip Filters for RF/Microwave Applications. 10.1002/0471221619. [13] X. Wu, S. Member, Y. Li, and S. Member, "High-Order Dual-Port Quasi-Absorptive Microstrip," IEEE Trans. Microw. Theory Tech., vol. PP, pp. 1–14, 2019.
- [14] Simpson, Dakotah & Gómez-García, Roberto & Psychogiou, Dimitra. (2019). Mixed-technology quasi-reflectionless planar filters: Bandpass, bandstop, and multi-band designs. International Journal of Microwave and Wireless Technologies. 11. 1-9.
- [15] J.-S. G. Hong and M. J. Lancaster, Microstrip filters for RF/microwave applications. John Wiley & Sons, 2004.
- [16] Kusama, Yusuke, and Ryota Isozaki."Compact and Broadband Microstrip Band-Stop Filters with Single Rectangular Stubs"2019. Applied Sciences 9, no. 2: 248.
- [17] D. J. Simpson, R. Gómez-García, and D. Psychogiou, "Mixed-technology quasi-reflectionless planar filters: Bandpass, bandstop, and multi-band designs," in International Journal of Microwave and Wireless Technologies, 2019, vol. 11, no. 5–6, pp. 466–474.
- [18] Wu, Gangxiong, Hao Wu, Wei Qin, Jin Shi, Wei Zhang, Longlong Lin, and Qian Li. 2023. "Design of a Switchable Filter for Reflectionless-Bandpass-to-Reflectionless-Bandstop Responses" Micromachines 14, no. 2: 424.
- [19] X.-B. Zhao, F. Wei, L. Yang and R. Gómez-Garcia, "Multi-Layer Second-Order Balanced Bandpass Filter with Differential-and Common-Mode Two-Port-Quasi-Reflectionless Behavior," 2023 IEEE MTT-S International Wireless Symposium (IWS), Qingdao, China, 2023, pp. 1-4.
- [20] Taghvaei, Abbas & Bayderkhani, Reza & Espahbodi, Maryam. (2022). Design and Fabrication of Adjustable Reflectionless Microstrip Diplexer for L-band. Progress In Electromagnetics Research C. 126. 173-181. 10.2528/PIERC22091203.
- [21] Al-Mudhafar, A. A. (2025). Design and fabrication reflectionless and Semireflectionless microwave diplexer. International Journal of Engineering in Computer Science, 7(2), 57–66. doi.org/10.33545/26633582.2025.v7.i2a.202
- [22] Alabedi, Y., Makki, S. V. A., & Alkhafaji, N. (2024). Five-pole wideband quasi-reflectionless interdigital BPF with second harmonic suppression. Engineering Research Express, 6(4), 045323. https://doi.org/10.1088/2631-8695/ad861e